ACS SENSORS

Article

Cite This: ACS Sens. 2018, 3, 2709−2715

pubs.acs.org/acssensors

Measuring Bone Biomarker Alkaline Phosphatase with Wafer-Scale Nanowell Array Electrodes

JuKyung Lee,[†,‡] Cameron T. Bubar,[†] Hi Gyu Moon,[‡,§] Jonghan Kim,[∥] Ahmed Busnaina,[†] HeaYeon Lee,[*,∥,⊥] and Sandra J. Shefelbine[*,†]

[†]Department of Mechanical and Industrial Engineering, College of Engineering, Northeastern University, Boston, Massachusetts 02115, United States

[‡]Korea Institute of Toxicology, Jeongeup-Si 56212, Republic of Korea

[§]Department of Chemistry and Biochemistry, University of California, Los Angeles, California 90095, United States

[∥]Department of Pharmaceutical Sciences, School of Pharmacy, Bouve College of Health Sciences, Northeastern University, Boston, Massachusetts 02115, United States

[⊥]Mara Nanotech New York, Inc., New York, New York 10031-9101, United States

Supporting Information

ABSTRACT: Biosensors that can analyze a single drop of biological fluid can overcome limitations such as extraction volume from humans or animals, ethical problems, time, and cost. In this work, we have developed a highly sensitive electrochemical (EC) biosensor based on a nanowell array (NWA) for the detection of alkaline phosphatase (ALP), a serum indicator of bone formation. The size of the electrode is 2 × 1 mm^2 and has over 10 million nanowells (400 nm diameter) arranged uniformly on the electrode surface. For detecting ALP, anti-ALP was immobilized and oriented on the NWA surface using a self-assembled monolayer and protein G. EC impedance spectroscopy (EIS) was used to determine the amount of ALP in 10 μL of sample. The impedance was calibrated with ALP concentration. The NWA has a linear dynamic range from 1 pg/mL to 100 ng/mL with a limit of detection (LOD) at 12 pg/mL. We used the sensor to measure the ALP in real mouse serum from 4, 10, and 20 weeks old mice and compared the results to the standard photometric assay. This work demonstrates the potential of EC NWA sensors to analyze a single drop of a real body fluid sample and to be developed for broad applications.

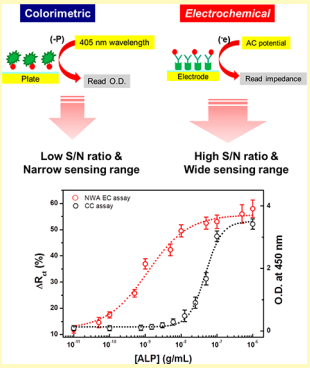

KEYWORDS: *nanowell array (NWA), immuno-affinity sensor, electrochemical impedance spectroscopy (EIS), alkaline phosphatase (ALP), bone formation indicator*

Monitoring of bone metabolic activity (bone formation and resorption) is critical for determining progression of bone disease or efficacy of treatment. Alkaline phosphatase (ALP) in blood serum is often used as a indicator of bone formation in numerous clinical pathologies: osteoporosis,[1,2] osteosarcoma,[3] Paget's disease,[4,5] and diabetes.[6] A recent study has shown that ALP concentrations in human blood serum varies with age, gender, and disease (normal range: 30−115 U/mL).[7] The ALP level in the blood is high during skeletal growth and periods of bone formation and decreases throughout life.[8] Currently, most tests for ALP levels in blood serum use the conventional photometric assay, which uses phosphatase reaction chemistry. In this photometric assay, ALP hydrolyzes *p*-nitrophenylphosphatase (PNPP), which is colorless, to *p*-nitrophenol (PNP), which is yellow and absorbs at 405 nm. The PNPP assay has a high limit of detection (LOD) value (10 μU) which describes the minimum concentration that can be detected when using body fluid samples because hemoglobin and other large cell debris affect optical density. Also, this assay needs fairly large sample volumes (e.g., 100−200 μL).

Enzyme-linked immunosorbent assay (ELISA) can also be used to measure ALP. This method uses antigen (Ag)−antibody (Ab) affinity and is also measured by a change in color. ELISA has a lower LOD value since it has a washing step to remove nonspecifically bound proteins in the origin sample. However, ELISA consists of several complex steps, including a labeling process with secondary antibody and fluorescence measurement, and consumes a larger sample volume (100−200 μL per sample). ELISA assays additionally require high maintenance cost, and some multiflex microplate readers occupy large space, which limits compatibility with the miniaturization. These techniques are therefore suitable for research studies and in clinical blood analysis laboratories but are difficult to adapt to real-time point-of-care measurements. There is a need for a rapid, accurate, easy to use, and inexpensive analysis of ALP quantification. Electrochemical (EC) immunosensors can be used as a point-of-care sensor

Received: October 25, 2018
Accepted: November 21, 2018
Published: November 21, 2018

DOI: 10.1021/acssensors.8b01298
ACS Sens. 2018, 3, 2709−2715

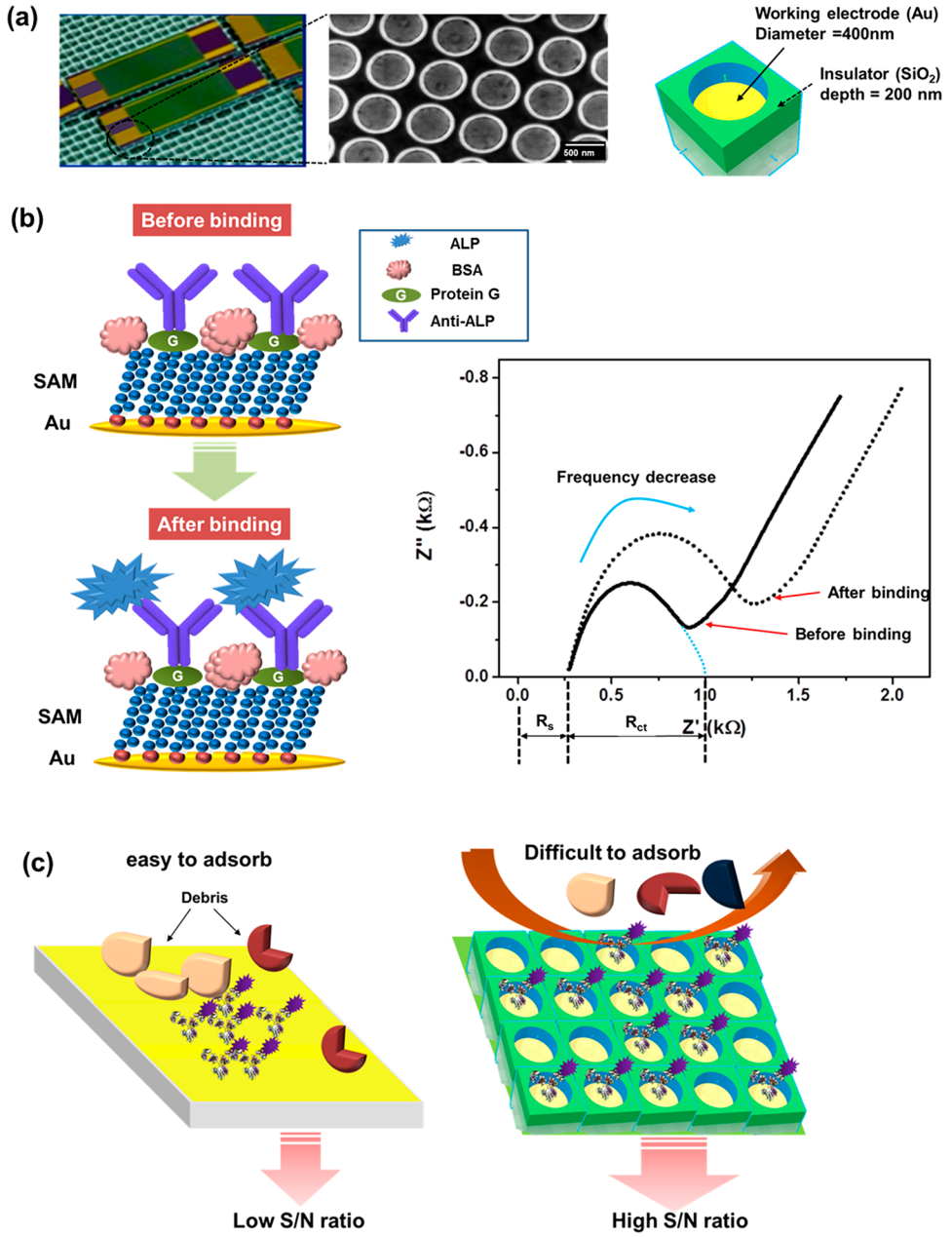

Figure 1. (a) SEM image of the overall NWA electrode and schematic image of a single well. NWA is fabricated on the large square region at the bottom of electrode (black circle). The yellow region is the Au working electrode, and the green region is the SiO_2 insulator. The scale bar is 500 nm. (b) Schematic illustration of ALP treatment in serum and impedance measurement. The ALP immunolayer was constructed on the NWA electrode (before binding); ALP binds to the ALP antibody (after binding), increasing the resistance of the electrode. This is measured in the Nyquist plot as an increase in charge transfer resistance value (the diameter of the semicircle). (c) Nonspecific adsorption occurs on flat electrode surfaces, resulting in low signal-to-noise; the small size of the NWA prevents nonspecific adsorption.

because measurement is rapid and inexpensive and has a low LOD.[9] In our previous work, we modified a screen printed electrode for detection of ALP and measured the impedance signal in PBS and serum. The screen printed electrode had a 5 ng/mL LOD in PBS and a 10 ng/mL of LOD in serum.[10] Though the electrode successfully detected ALP, the microelectrode posed two primary limitations: (1) a large surface area still required a larger volume of sample (100 μL), and (2) the microsize working area is affected by solution resistance, impurities, and nonspecific binding more than a nanoelectrode.[11] These effects resulted in a sensor with low reliability and limited accuracy even though we successfully measured ALP in a range 1.8 to 1000 ng/mL. For these reasons, there is a need for a reliable sensor that allows direct, easy quantification of bone biomarkers with high sensitivity and specificity.

In this paper, we developed an ALP EC immunosensor using a nanowell array (NWA) electrode with high sensitivity, selectivity, and signal-to-noise ratio (S/N ratio) and requiring only 10 μL of sample volume per sample based on EC impedance spectroscopy (EIS). Finally, NWA's effectiveness was demonstrated by comparing a standard colorimetric assay and by detection of ALP with low levels in real mouse serum extracted at different ages.

DOI: 10.1021/acssensors.8b01298
ACS Sens. 2018, 3, 2709−2715

EXPERIMENTAL SECTION

Materials. Potassium ferricyanide [$K_3Fe(CN)_6$], ethanolamine hydrochloride, 11-mercapto undecanoic acid (11-MUA), N-(3-(dimethylamino)propyl)-*N*′-ethylcarbodiimide (EDC), *N*-hydroxysuccinimide (NHS), bovine serum albumin (BSA), sodium citrate dihydrate, phosphate buffer saline (PBS), mouse albumin lyophilized powder, and fetal bovine serum (FBS) were purchased from Sigma-Aldrich (St. Louis, USA). Protein G (PG) was purchased from Thermoscientific (Cambridge, USA), and C57BL6 mouse serum was purchased from Innovative reserach (Novi, USA). Mouse alkaline phosphatase (ALP) protein (2910-AP-010) and goat polyclonal anti-ALP antibody (AF-2910) was purchased from R&D systems (Minneapolis, USA). Conventional colorimetric (CC) assay was performed with an ALP colorimetric assay kit (ab83369) purchased from Abcam (Cambridge, USA).[12−14]

Wafer-Scale NWA Patterning. The NWA patterning was made by KrF stepper as previously detailed.[15] Briefly, (1) the Si wafer was cleaned using a sulfuric peroxide mixture. (2) A 300-nm-thick silicon dioxide (SiO_2) layer was deposited. (3) Both a 30 nm Ti (adhesion layer) and 300-nm-thick Au layer were deposited. (4) Photoresist was deposited. (5) Whole electrode morphology was made by mask alignment. (6) Ti/Au layers were removed by etching. (7) Photoresist was removed. (8) A second SiO_2 layer with a thickness of 200 nm was deposited. (9) A second photoresist was deposited. (10) The KrF stepper process was used for patterning NWA. (11) The SiO_2 layer was etched, and photoresist was removed.

Preparation of Immunolayer on NWA. NWA electrodes were fabricated by the KrF stepper process (briefly outlined above), resulting in an array of 2500 × 5000 nanowells (diameter = 400 nm, depth = 200 nm; Figure 1a). AFM profiling verified our NWA specification (Figure S1). The electrodes were first treated with a self-assembled monolayer (SAM) to allow covalent bonding with proteins. To create the SAM, NWA electrodes were treated with acetone, cleaned with ethanol and DI water, and dried in a stream of N_2. Electrodes were then incubated in 10 mM 11-mercapto undecanoic acid (11-MUA) dissolved in anhydrous ethanol for 1 h at room temperature. Next, equal parts 50 mM EDC and 50 mM NHS in pH 4.5 sodium citrate buffer were used to activate the carboxyl groups on the SAM. Next, 10 μg/mL protein G (PG) was immobilized on the SAMs by covalent bonding for 1 h at room temperature (RT) in order to increase antibody (Ab) density and ensure Ab orientation. The unreacted activated carboxyl groups were blocked by 1 M ethanolamine for 10 min at RT. Finally, a solution of 10 μg/mL anti-ALP antibody was immobilized by PG-antibody affinity, followed by BSA blocking (1 mg/mL for 30 min), which deactivates nonantibody area in the NWA preventing nonspecific binding. After that, a 5 μL volume of antigen in different solutions (PBS, 10% diluted FBS, undiluted mouse blood serum) was dropped on the NWA and incubated for 30 min at RT. After washing using 0.05% PBS tween 20 (three times repeated), NWA was dried using nitrogen (99% purity) and EC measurement performed. The schematic of the sensor is shown in Figure 1b.

Electrochemical Analysis of NWA. An EC assay to quantify ALP based on impedance measurement was performed with a three-electrode system, including a working electrode (WE: NWA), a counter electrode (CE: Pt electrode), and a reference electrode (RE: Ag/AgCl/KCl). All three electrodes were connected to a potentiostat (ALS 600A, Texas, USA) that measured impedance. All three electrodes were immersed into an electrolytic conducting solution, 5 mM $K_3Fe(CN)_6$ + 0.1 M KCl in pH 7.4 PBS at RT. Impedance spectra were recorded from 1 kHz to 0.1 Hz. Then, 50 mV AC signal amplitudes were applied with fixing the DC potential at 0 V. After measurement, data were fit by using Z-view software (Scribner Associates Inc., USA). As shown in Figure 1b, impedance data can be analyzed with a Nyquist plot. Nyquist plots were generated by plotting the imaginary (out of phase, *y*-axis component) versus the real (in phase, *x*-axis component) values.[16] The diameter of the semicircle, which corresponds to the charge transfer resistance (R_{ct}), was used for determining the analyte (ALP) concentration. When the ALP was bound to the ALP antibody, the biomolecule layers on the electrode became denser, making it more difficult for electron transfer from electrolyte solution to the electrode. Most biomolecules have low dielectric constants (between 2 and 20),[17] which means they are nonconductive materials. They act like a resistive layer on the electrode, so electrons from the electrolyte cannot easily pass through the resistive layer on the electrode surface. The charge transfer resistance R_{ct} increased (diameter of the semicircle increased) with the increasing binding rate between ALP and ALP antibody.

In this work, ΔR_{ct} (%) was calculated to quantify ALP, and it was determined by

$$\Delta R_{ct}\ (\%) = \frac{\Delta R_{ct}}{R_{ct}^{BSA}} \times 100 = \frac{R_{ct}^{Ab-Ag} - R_{ct}^{BSA}}{R_{ct}^{BSA}} \times 100 \quad (1)$$

where R_{ct}^{Ab-Ag} is the value of the R_{ct} value after ALP as Ag binds to ALP antibody on the NWA surface. R_{ct}^{BSA} is the value after BSA adsorption to block nonspecific binding as a baseline. To calibrate EC measurements, concentrations of ALP from 1 pg/mL and 1 μg/mL were measured in PBS. After calibration in PBS, ALP was spiked in 10% fetal bovine serum (diluted 1:9 with PBS) also from 1 pg/mL and 1 μg/mL. Testing in fetal bovine serum (FBS) determined the effects of nonspecific binding.[18] After measuring the sensor's performance in FBS, undiluted mouse blood serum was tested as "real sample" analysis indicates the potential for direct translation of this technique to the lab. All tests used the CC assay as the photometric validation. CC tests were carried out according to the manufacturer's instructions. The CC calibration curve was estimated using the positive and negative samples included in the CC kit. ALP concentration was determined by EC measurement (eq 1) mapped onto the calibration curve. ALP Ab immobilized NWA was used as a positive control, and NWA without any ALP Ab (only BSA blocking) was used as a negative control in mice serum analysis.

Mouse Serum Collection. C57/Bl6 mice (n = 18) were obtained from Jackson Laboratories (Bar Harbor, USA) with six mice for each of the following age groups: 4 weeks, 10 weeks, and 20+ weeks. All experiments were approved by the Institutional Animal Care and Use Committee and conducted according to the guidelines of Association for Assessment and Accreditation of Laboratory Animal Care International. After sacrifice, the blood was extracted via cardiac exsanguination and subsequently was centrifuged in order to isolate the serum. The serum was stored at −80 °C until analysis.

Working Cycle of the ALP Immunosensor. To assess the number of working cycles of the NWA electrode, 100 pg/mL of ALP in serum was applied to the NWA electrode. The current was measured in a 5 mM $K_3Fe(CN)_6$ solution, then washed with PBS three times. After washing, the electrode was dipped in 10 mM NaOH for 1 min at RT to remove the ALP but keep the ALP antibody, washed again using PBS, and reused for the same procedure. In this experiment, regeneration was performed by comparing the peak current of ALP Ab and peak current of attaching 100 pg/mL ALP in 10% diluted serum. The electrode was immersed in (1) 10 mM glycine buffer (low pH conditions: pH 2.4) for 3 min and (2) 10 mM NaOH (high pH conditions: pH 10.3) for 3 min. Then, faradaic current by SWV was measured from 0.6 V to −0.2 V to observe regeneration efficacy. This process was repeated until regeneration efficiency was less than 80%.

$$\text{regeneration efficiency}(\%) = \left(\frac{I_{Ag\text{-}Ab} - I_{reg}}{I_{Ag\text{-}Ab} - I_{Ab}}\right) \times 100\%$$

where $I_{Ag\text{-}Ab}$ is the current signal of the electrode at which ALP was bound to the ALP antibody, I_{reg} is the current signal of the electrode after regeneration, and I_{Ab} is the current signal of the electrode at which the ALP antibody only was attached.

Methods in Statistics. All assays (EC, CC) were run five times, and mean and standard deviation were calculated at each concentration to generate the calibration curve. Each replicate was measured with a new NWA electrode. The electrolyte ($K_3Fe(CN)_6$)

DOI: 10.1021/acssensors.8b01298
ACS Sens. 2018, 3, 2709−2715

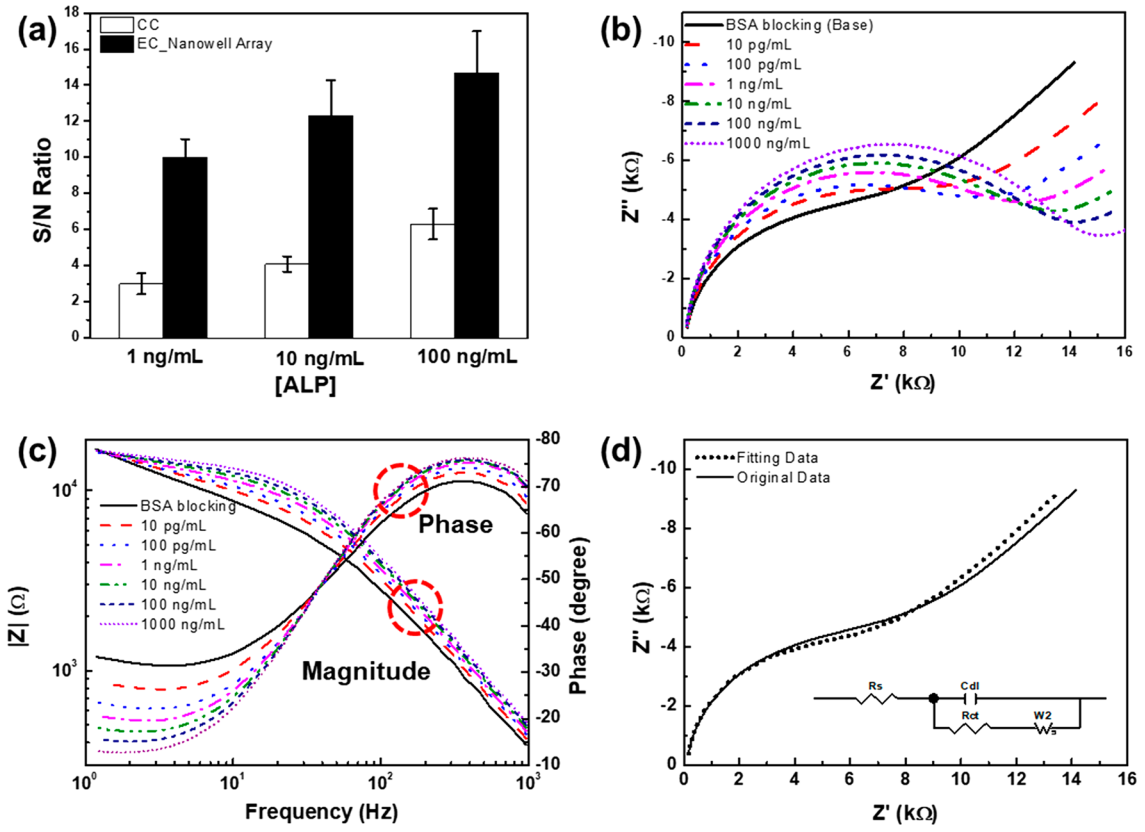

Figure 2. (a) Comparison of the S/N ratio of CC and EC NWA electrode. The EC NWA measurements had a higher S/N ratio compared to CC measurements. (b) Representative Nyquist plots of ALP with sensing range from 1 pg/mL to 100 ng/mL. (c) Bode plot of ALP with sensing range from 1 pg/mL to 100 ng/mL. The curves in the upper circle represent the phase of impedance and in the lower circle represent the magnitude of impedance. (d) Fitting result of impedance plot of ALP antibody immobilized on NWA electrode with a Randles circuit.

was newly made at each time measurement to maintain fresh conditions. Nonlinear curve fitting was performed with Origin 8.0.

RESULTS AND DISCUSSION

Overall, we found that the conformational structure of the NWA allowed sensing of ALP in undiluted serum with high sensitivity and selectivity. We first determined the S/N ratio for the CC and the EC NWA electrode at ALP concentrations of 1, 10, and 100 ng/mL (n = 5). The S/N ratio was calculated as the ratio of analyte signal (anti-ALP immobilized electrode) to the blank signal (no analyte in PBS).[19−21] As shown in Figure 2a, EC NWA demonstrated a higher S/N ratio than the CC assay (CC's S/N ratio is 3.02 ± 0.58 at 1 mg/mL, 4.14 ± 0.43 at 10 ng/mL, and 6.32 ± 0.85 at 100 ng/mL, and NWA's S/N ratio is 9.78 ± 1.02 at 1 ng/mL, 11.96 ± 1.98 at 10 ng/mL, and 14.35 ± 2.31 at 100 ng/mL, respectively). Figure 2b shows the Nyquist plot for the NWA electrodes using ALP spiked in PBS as an antigen at various concentrations. R_{ct} increased with increasing ALP concentration (diameter of the circle increases). R_{ct} indicates the dielectric behavior of the electrode; at high concentrations, more ALP is bound to the sensor, making a denser, thicker insulation layer that can better store charge than at low concentrations.[22]

The Bode plot in Figure 2c shows |Z| increases with increasing ALP concentration, particularly at frequencies below 40 Hz for which the signal is dominated by the dielectric behavior of the electrode surface. These results matched with cyclic voltammetry (CV) and square wave voltammetry (SWV) data (Figure S2). We performed the impedance measurements from 10 kHz (10^4 Hz) to 0.1 Hz; however, there was no difference in the high frequency region (over 1 kHz). Only in the very low frequency region (<40 Hz) did the impedance increase with increasing concentrations of ALP. We modeled the immunosensor system as a Randles circuit[23,24] (a resistor in series with a parallel capacitor and resistor) in order to characterize capacitance (C_{dl}), Warburg's impedance (W), the electrolyte's solution resistance (R_s), and the charge transfer resistance (R_{ct}). Typically in an EC sensor, C_{dl} and R_{ct} values are used to quantify the analyte because these values change with increasing analyte concentrations. Figure 2d shows the experimental data with the model fit. C_{dl} is 477.72 nF, R_{ct} is 5676 Ω, R_s is 157.2 Ω, and W is 135.12 Ω, respectively (χ^2 = 0.001).

Sensor Sensitivity and Dynamic Range. Figure 3 shows the results of ALP in PBS based on the NWA EC and CC assay. Comparing the NWA sensor and CC responses indicated that the NWA had a lower LOD of 12 pg/mL, n = 3 (LOD of CC: 5.4 ng/mL, n = 3) and wider detection range than CC from 12 pg/mL to 1 μg/mL (range of CC: 5.4 ng/mL to 1 μg/mL). In this calibration curve, LOD is estimated by gathering the signal of the zero concentrations value plus 3 times its standard deviation.[14]

The EC sensor's selectivity was determined in serum in order to demonstrate the sensor's effectiveness in the presence of other proteins, cell debris, and albumin, which are large components in serum. We used mouse leptin as a nonspecific binding protein against the ALP specific binding protein. R_{ct} did not change with incubation of leptin in serum on the NWA

DOI: 10.1021/acssensors.8b01298
ACS Sens. 2018, 3, 2709−2715

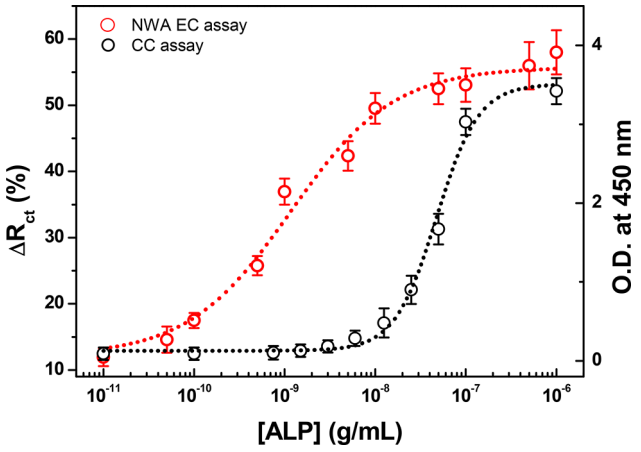

Figure 3. (a) Calibration curve of ALP by NWA EC measurement (red) and CC measurement (black). In both of them, ALP is spiked in pure buffer (10 mM PBS, pH 7.4). In the EC measurement, 5 mM $K_3Fe(CN)_6$ in PBS was used as the electrolyte (n = 5).

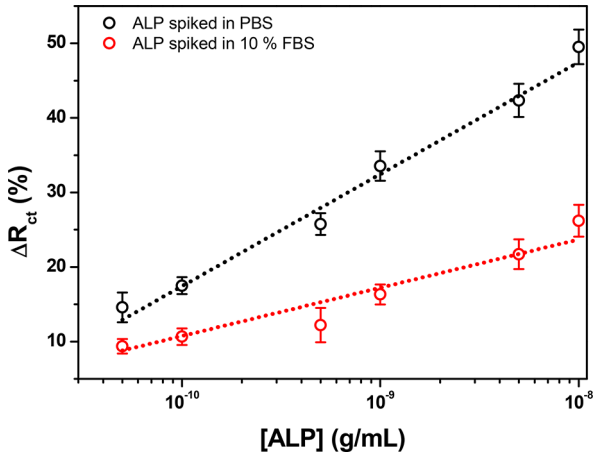

Figure 4. Calibration curve and linear property based on NWA EC measurement with range from 50 pg/mL to 10 ng/mL. ALP spiked in PBS (black circle) and 10% diluted FBS (red circle; n = 5).

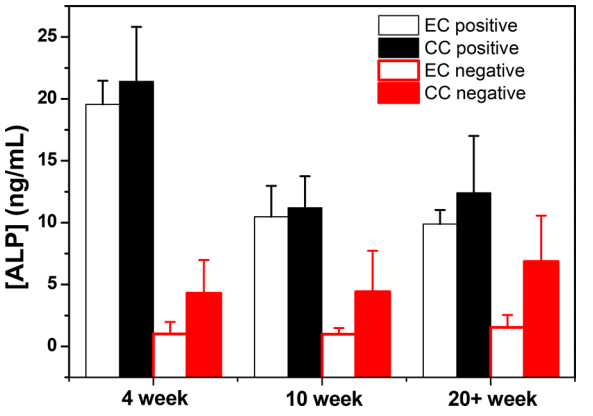

Figure 5. ALP quantification using undiluted mouse serum which was collected from specimens at 4, 10, and 20 week ages. Unfilled bar is the result of NWA EC and filled bar is the result of CC assay (n = 5).

Table 1. Comparison of Results from NWA EC and CC Assay

sample	[ALP] by CC (ng/mL)	[ALP] by EC (ng/mL)	RSD (%)
4 week	21.41 ± 3.41	19.56 ± 1.96	9.46
10 week	11.23 ± 2.54	10.47 ± 2.51	7.26
20+ week	8.42 ± 4.59	7.89 ± 1.13	6.72

(Figure S3a). Figure S3b shows the R_{ct} ratio in the presence of ALP and in the presence of leptin in serum at 0.1, 1, 10, and 100 ng/mL, respectively. There were no significant differences between the antibody (ALP) layer with and without leptin, indicating that the NWA EC sensor has high selectivity even in serum. ALP was additionally calibrated in 10% FBS (in which there are other proteins but insignificant amounts of ALP).[25] R_{ct} increased with increasing ALP, and it shows a similar result to ALP measured in pure PBS buffer (Figure S4). Comparing buffer and serum calibrations, there are two differences: (1) The diffusion region (linear region with upward slope) at low frequencies disappeared in serum. We assumed this effect occurs for the cell debris effect. Serum contains cell debris, which is adsorbed in the SiO_2 region by physical adsorption. This does not affect the signal because SiO_2 is an insulator. However, the diffusion process is affected by the cell debris found in serum because most of the cell debris has a negative surface charge because of the phospholipid membrane. Electrons in the electrolyte solution cannot pass through easily to the electrode (repulsion). Cell debris may additionally adsorb on the electrode, creating a blocking layer, so electrons cannot easily pass through. (2) The R_{ct} of the Ab layer is increased (10.46 kΩ → 21.87 kΩ), which is likely caused by nonspecific binding. Even with these disadvantages in serum analysis, our NWA shows enough selectivity, as already shown in Figure S3. Under serum conditions, the NWA EC still maintained a linear range from 50 pg/mL to 10 ng/mL with a sensitivity of $[0.0647]\Delta R_{ct} \times (\log [g/mL])$ despite being lower than the sensitivity in PBS (Figure 4).

Figure 5 and Table 1 show the results of the NWA EC and CC assay using blood serum from different aged mice. Both NWA EC and CC results indicated that the 4 week old mice had a higher ALP serum concentration than that of older ages, which is expected due to skeletal growth at the young age. The concentration by both methods in mice serum with different ages matched to within 10%.

Previous studies about the relationship between ALP and age have shown that ALP is higher in young mice than in old mice.[26] Our results agree with these findings, with higher ALP in the 4-week group than in any other groups. The two methods we used measured similar ALP concentrations, but their operation procedure is clearly different: (1) The NWA EC assay uses specific binding of Ab-Ag, while CC assays use the dephosphorylation method by inserting labeling chemicals (p-NPP). (2) A washing step which can remove nonspecific binding is performed in the EC but not in the CC assay, and (3) NWA EC used 5 μL of volume per test but CC used 200 μL per test. These differences affected the negative control data as shown in Figure 5. Negative control data of the CC assay are higher than the NWA EC control data, which could be due to the nonspecific binding that is not washed away in the CC test. The ratio of positive control to the negative control (P/N ratio) in 4 weeks was 10.87 NWA EC vs 5.08 CC, in 10 weeks was 13.51 NWA EC vs 2.53 CC, and in 20+ week was 5.16 NWA EC vs 2.18 CC. The NWA EC sensor maintained a high S/N ratio since it used specific binding of Ab-Ag and the presence of a washing step to remove nonspecific binding.

DOI: 10.1021/acssensors.8b01298
ACS Sens. 2018, 3, 2709−2715

Compared to other types of ALP NWA EC sensing, not just the CC assay,[10,25,27−32] this NWA EC method has the advantages of being a simple procedure, consuming an extremely low volume of sample, having a low LOD and wide linear range, and having applicability to blood serum (Table 2).

Table 2. Fluorescent and EC Assay Reported in the Literature for the Determination of ALP (ITO, Indium Tin Oxide; CNT, Carbon Nanotube; F, Fluorescent; DNA, Deoxyribonucleic Acid)

analysis method	method	LOD	linear range	ref
8-quinolyl phosphate	F	1 U/L	1−16 IU/L	27
enzyme linked immunosorbent assay (ELISA)	F	5 U/L	5−180 U/L	28
graphene QDs	F	0.017 nM (0.3 U/L)	0.05−2.5 nM 5−10 nM	29
screen printed Au electrode	EC	5 ng/mL (PBS) 10 ng/mL (serum)	10^{-9} to 10^{-5} g/mL	10
CNT electrode	EC	0.25 U/L	0.5−600 U/L	30
glassy carbon electrode	EC	0.03 U/L	0.03−300 U/L	31
Au flat microelectrode	EC	1 ng/mL	1−400 ng/mL	32
CeO_2 nanocrystal	EC	0.002 U/L	0.01−150 U/L	33
Au nanowell array electrode	EC	12 pg/mL	10^{-12} to 10^{-9} g/mL 10^{-8}∼10^{-5} g/mL	this work

The NWA EC assay has a low LOD (NWA EC: 5.4 pg/mL vs CC: 5.8 ng/mL) and wider range (NWA EC: 10 pg/mL to 1 μg/mL vs CC: 8 ng/mL ∼ 14 μg/mL) than the CC assay. However, in the 8 ng/mL to 30 μg/mL range (which is the physiological range), the conventional method is more sensitive than the NWA EC assay. These results demonstrate that the NWA EC is more effective at extremely lower ranges, and the CC method is effective at higher concentration ranges. Recently, many research groups have developed biosensors for detecting biomarkers in urine, saliva, and sweat as body fluids, which are more easily obtained, but contain vary low concentrations of analyte. The NWA EC holds potential for biomarker sensing in such applications as it is sensitive at low concentrations and uses small sample volumes.

ALP NWA Biosensor Regeneration. Regeneration in NaOH dissociates the ALP antibody−ALP antigen complex. Most of the antibody−antigen interactions can be disrupted by low pH conditions or high salt and high pH conditions. We found the glycine wash (low pH) did not change the binding resistance, indicating there was likely no ALP-antibody dissociation. However, the NaOH wash restored the resistance to its prebinding value. As shown in Figure S5a,b, the Δ peak current of 5 times regeneration is similar to the initial Δ peak current in 10 mM NaOH. However, the Δ peak current is dramatically increased after five or more regenerations (Figure S5c). The NaOH wash possibly affected the protein G and BSA protein on the NWA electrode after 5 times of regeneration (Figure 6). Our NWA can be reused for 5 working cycles.

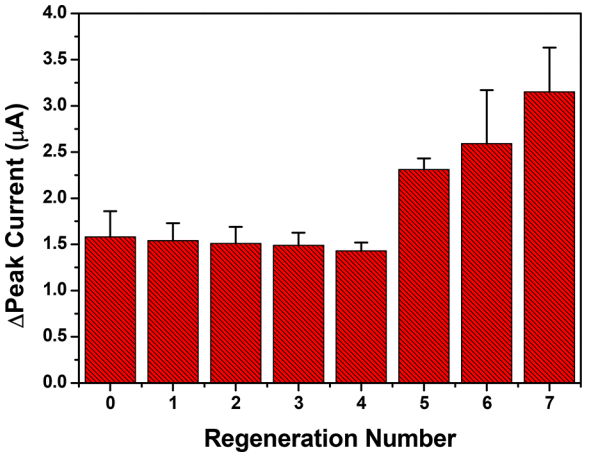

Figure 6. Regeneration of NWA EC sensor by immersing in 10 mM NaOH for 3 min. Δ Peak current is calculated by SWV before and attaching ALP at 100 pg/mL in 10% diluted serum, repeatedly. SWV was performed in 5 mM $K_3Fe(CN)_6$ in PBS (n = 5).

CONCLUSIONS

We demonstrated that the NWA EC enables detection of ALP at low concentrations in undiluted blood serum. Currently, most of the ALP detection assays use optical methods such as fluorescence or ELISA, which typically require sample volumes of 200 μL, cannot be used with whole blood, and are currently not portable given the equipment required. The advantages of the NWA EC sensor are the short analysis time, high S/N ratio, low LOD, and use of very little sample (5 μL). In addition, the potential for miniaturization of required electronics could allow a portable and simple point-of-care analysis system. This demonstrates the potential of NWA EC sensors to be used in detection of other biomarkers in blood, serum, and urine or even sweat or saliva as the LOD is so low. NWA EC sensors will become a powerful tool for point-of-care biomarker assessment.

ASSOCIATED CONTENT

Supporting Information

The Supporting Information is available free of charge on the ACS Publications website at DOI: 10.1021/acssensors.8b01298.

Atomic force microscopy (AFM) image of NWA and line profile (Figure S1) and CV and SWV data (Figure S2), selectivity of NWA EC (Figure S3), Nyquist plot by NWA EC assay using ALP spiked in FBS (Figure S4), regeneration signal (Figure S5) (PDF)

AUTHOR INFORMATION

Corresponding Authors

*Tel.: +1-617-373-3199. E-mail: he.lee@northeastern.edu.
*E-mail: s.shefelbine@neu.edu.

ORCID

JuKyung Lee: 0000-0002-2751-8112
Ahmed Busnaina: 0000-0001-8565-385X

Author Contributions

S.J.S. and H.L. contributed equally as corresponding authors.

Notes

The authors declare no competing financial interest.

DOI: 10.1021/acssensors.8b01298
ACS Sens. 2018, 3, 2709−2715

■ ACKNOWLEDGMENTS

This research was supported by the Basic Science Program of the National Research Foundation of Korea (NRF), funded by the Ministry of Education, Science and Technology (2014-052607).

■ REFERENCES

(1) Cabral, H. W. S.; Andolphi, B. F. G.; Ferreira, B. V. C.; Alves, D. C. F.; Morelato, R. L.; Chambo Filho, A.; Borges, L. S. The use of biomarkers in clinical osteoporosis. *Revista da Associação Médica Brasileira* **2016**, *62* (4), 368−376.

(2) Bandeira, F.; Costa, A. G.; Soares Filho, M. A.; Pimentel, L.; Lima, L.; Bilezikian, J. P. Bone markers and osteoporosis therapy. *Arq. Bras. Endocrinol. Metabol.* **2014**, *58* (5), 504−513.

(3) Du, W. X.; Duan, S. F.; Chen, J. J.; Huang, J. F.; Yin, L. M.; Tong, P. J. Serum bone-specific alkaline phosphatase as a biomarker for osseous metastases in patients with malignant carcinomas: a systematic review and meta-analysis. *J. Cancer Res. Ther* **2014**, *10* (7), 140.

(4) Deftos, L. J.; Wolfert, R. L.; Hill, C. S. Bone alkaline phosphatase in Paget's disease. *Horm. Metab. Res.* **1991**, *23* (11), 559−561.

(5) Al Nofal, A. A.; Altayar, O.; BenKhadra, K.; Qasim Agha, O. Q.; Asi, N.; Nabhan, M.; Prokop, L. J.; Tebben, P.; Murad, M. H. Bone turnover markers in Paget's disease of the bone: a systematic review and meta-analysis. *Osteoporosis Int.* **2015**, *26* (7), 1875−1891.

(6) Starup-Linde, J.; Vestergaard, P. Biochemical bone turnover markers in diabetes mellitus—a systematic review. *Bone* **2016**, *82*, 69−78.

(7) Saif, M. W.; Alexander, D.; Wicox, C. M. Serum alkaline phosphatase level as a prognostic tool in colorectal cancer: a study of 105 patients. *J. Appl. Res.* **2005**, *5* (1), 88−95.

(8) Pietschmann, P.; Rauner, M.; Sipos, W.; Kerschan-Schindl, K. Osteoporosis: an age-related and gender-specific disease−a mini-review. *Gerontology* **2009**, *55* (1), 3−12.

(9) Liu, S.; Wu, X.; Zhang, D.; Guo, C.; Wang, P.; Hu, W.; Li, X.; Zhou, X.; Xu, H.; Luo, C.; Zhang, J.; Chu, J. Ultrafast dynamic pressure sensors based on graphene hybrid structure. *ACS Appl. Mater. Interfaces* **2017**, *9* (28), 24148−24154.

(10) Lee, J.; Bubar, C. T.; Busnaina, A.; Shefelbine, S. J.; Lee, H. Standardization of a bone formation biomarker quantification using screen printed electrodes. *Appl. Spectrosc. Rev.* **2016**, *51* (7−9), 753−761.

(11) Wightman, R. M. Probing cellular chemistry in biological systems with microelectrodes. *Science* **2006**, *311* (5767), 1570−1574.

(12) Kim, I. R.; Kim, S. E.; Baek, H. S.; Kim, B. J.; Kim, C. H.; Chung, I. K.; Park, B. S.; Shin, S. H. The role of kaempferol-induced autophagy on differentiation and mineralization of osteoblastic MC3T3-E1 cells. *BMC Complementary Altern. Med.* **2016**, *16* (1), 333.

(13) Gardin, C.; Ferroni, L.; Piattelli, A.; SIvolella, S.; Zavan, B.; Mijiritsky, E. (2016). Non-washed resorbable blasting media (NWRBM) on titanium surfaces could enhance osteogenic properties of MSCs through increase of miRNA-196a and VCAM1. *Stem Cell Rev. Rep* **2016**, *12* (5), 543−552.

(14) Lauria, I.; Kramer, M.; Schröder, T.; Kant, S.; Hausmann, A.; Böke, F.; Leube, R.; Telle, R.; Fischer, H. Inkjet printed periodical micropatterns made of inert alumina ceramics induce contact guidance and stimulate osteogenic differentiation of mesenchymal stromal cells. *Acta Biomater.* **2016**, *44*, 85−96.

(15) Lee, J.; Cho, S.; Lee, J.; Ryu, H.; Park, J.; Lim, S.; Oh, B.; Lee, C.; Huang, W.; Busnaina, A.; Lee, H. Wafer-scale nanowell array patterning based electrochemical impedimetric immunosensor. *J. Biotechnol.* **2013**, *168* (4), 584−588.

(16) Basics of electrochemical impedance spectroscopy. *Appl. Note AC*; Gamry Instruments, 2010; vol *286*, pp R491−R497.

(17) Lee, J. K.; Noh, G. H.; Pyun, J. C. Capacitive immunoaffinity biosensor by using diamond-like carbon (DLC) electrode. *BioChip J.* **2009**, *3* (4), 287−292.

(18) Zhao, S.; Yang, W.; Lai, R. Y. (2011). A folding-based electrochemical aptasensor for detection of vascular endothelial growth factor in human whole blood. *Biosens. Bioelectron.* **2011**, *26* (5), 2442−2447.

(19) Kim, P.; Lee, B. K.; Lee, H. Y.; Kawai, T.; Suh, K. Y. Molded Nanowell Electrodes for Site-Selective Single Liposome Arrays. *Adv. Mater.* **2008**, *20* (1), 31−36.

(20) Lee, B. K.; Lee, H. Y.; Kim, P.; Suh, K. Y.; Kawai, T. Nanoarrays of tethered lipid bilayer rafts on poly (vinyl alcohol) hydrogels. *Lab Chip* **2009**, *9* (1), 132−139.

(21) Pan, Y.; Sonn, G. A.; Sin, M. L.; Mach, K. E.; Shih, M. C.; Gau, V.; Wong, P. K.; Liao, J. C. Electrochemical immunosensor detection of urinary lactoferrin in clinical samples for urinary tract infection diagnosis. *Biosens. Bioelectron.* **2010**, *26* (2), 649−654.

(22) Yang, L.; Li, Y.; Erf, G. F. Interdigitated Array Microelectrode-Based Electrochemical Impedance Immunosensor for Detection of Escherichia coli O157: H7. *Anal. Chem.* **2004**, *76* (4), 1107−1113.

(23) Janek, R. P.; Fawcett, W. R.; Ulman, A. Impedance spectroscopy of self-assembled monolayers on Au (111): sodium ferrocyanide charge transfer at modified electrodes. *Langmuir* **1998**, *14* (11), 3011−3018.

(24) Suni, I. I. Impedance methods for electrochemical sensors using nanomaterials. *TrAC, Trends Anal. Chem.* **2008**, *27* (7), 604−611.

(25) Kim, H. J.; Kwak, J. (2005). Electrochemical determination of total alkaline phosphatase in human blood with a micropatterned ITO film. *J. Electroanal. Chem.* **2005**, *577* (2), 243−248.

(26) Hatayama, K.; Nishihara, Y.; Kimura, S.; Goto, K.; Nakamura, D.; Wakita, A.; Urasoko, Y. (2011). Alkaline phosphatase isoenzymes in mouse plasma detected by polyacrylamide-gel disk electrophoresis. *J. Toxicol. Sci.* **2011**, *36* (2), 211−219.

(27) de Vries, E. M.; Wang, J.; Leeflang, M. M.; Boonstra, K.; Weersma, R. K.; Beuers, U. H.; Geskus, R. B.; Ponsioen, C. Y. Alkaline phosphatase at diagnosis of primary sclerosing cholangitis and 1 year later: evaluation of prognostic value. *Liver Int.* **2016**, *36* (12), 1867−1875.

(28) Hung, H. Y.; Chen, J. S.; Tang, R.; Hsieh, P. S.; You, Y. T.; You, J. F.; Chiang, J. M.; Yeh, C.-Y.; Tasi, W.-S. Preoperative alkaline phosphatase elevation was associated with poor survival in colorectal cancer patients. *International journal of colorectal disease* **2017**, *32* (12), 1775−1778.

(29) Zhu, Y.; Wang, G.; Jiang, H.; Chen, L.; Zhang, X. One-step ultrasonic synthesis of graphene quantum dots with high quantum yield and their application in sensing alkaline phosphatase. *Chem. Commun.* **2015**, *51* (5), 948−951.

(30) Simão, E. P.; Frías, I. A.; Andrade, C. A.; Oliveira, M. D. Nanostructured electrochemical immunosensor for detection of serological alkaline phosphatase. *Colloids Surf., B* **2018**, *171*, 413−418.

(31) Liu, Y.; Xiong, E.; Li, X.; Li, J.; Zhang, X.; Chen, J. Sensitive electrochemical assay of alkaline phosphatase activity based on TdT-mediated hemin/G-quadruplex DNAzyme nanowires for signal amplification. *Biosens. Bioelectron.* **2017**, *87*, 970−975.

(32) Zhao, M.; Zhang, S.; Chen, Z.; Zhao, C.; Wang, L.; Liu, S. Allosteric kissing complex-based electrochemical biosensor for sensitive, regenerative and versatile detection of proteins. *Biosens. Bioelectron.* **2018**, *105*, 42−48.

(33) Jin, L. Y.; Dong, Y. M.; Wu, X. M.; Cao, G. X.; Wang, G. L. Versatile and amplified biosensing through enzymatic cascade reaction by coupling alkaline phosphatase in situ generation of photoresponsive nanozyme. *Anal. Chem.* **2015**, *87* (20), 10429−10436.

DOI: 10.1021/acssensors.8b01298
ACS Sens. 2018, 3, 2709−2715